한국표면공학회지
Journal of the Korean Institute of Surface Engineering
Vol. 29, No. 3, Jun. 1996
<연구논문>

플라즈마 용사에 의한 열벽코팅의 상변태가 내구성에 미치는 영향

이의열

안동대학교 재료공학과, 경북안동시 송천동388

The Effect of the Phase Transformations on the Durability of the Plasma Sprayed Thermal Barrier Coatings

E. Y. Lee

Dept. of Materials Science and Engineering Andong National University,
388 Songchun-dong, Andong, Kyungbuk, Korea

초 록

플라즈마 용사된 열벽코팅의 수명을 평가하기 위하여 여러가지 양의 CeO_2(16,18,20,22,24 그리고 26 wt.% CeO_2)를 포함하는 지르코니아 코팅에 대한 상분석이 행하여 졌다. 플라즈마 용사된 후 16 및 18 wt.% CeO_2를 포함하는 지르코니아 코팅에서는 비평형 tetragonal 상 만이 생성되었으나 20-26 wt.% CeO_2를 포함하는 지르코니아 코팅에서는 비평형 tetragonal 및 cubic 상의 혼합상이 관찰되었다. 열순환 산화시험 동안에는 비평형 tetragonal 및 cubic 상은 평형 tetragonal 및 cubic 상으로 변태하였다. 평형 tetragonal 상의 일부는 열순환 산화시험의 냉각과정 중에 monoclinic 상으로 변태하였다. 그리고 16 wt.% CeO_2를 포함하는 지르코니아 코팅은 다른 조성의 지르코니아 코팅보다 열순환 산화시험 동안 더 많은 monoclinic 상이 생성되었으며 세라믹 코팅 수명이 짧았다.

1. Introduction

Two layer thermal barrier coating(TBC) systems consisting of ZrO_2 based ceramic coatings on an MCrAlY(M=Ni and/or Co) bond coats are of prime interest because of their ability to improve performance and efficiency of gas turbine engine by allowing higher combustion gas temperature or reduced cooling air flow[1-4]. The most durable ceramic materials used for the TBCs in a cyclic high temperature environment were found to be partially stabilized zirconia (PSZ) with yttria[5-8].

During cyclic oxidation, PSZ coatings can undergo substantial expansion on cooling and contraction on heating due to a tetragonal(T)-monoclinic(M) transformation[9-11]. The dilatation and shear strains associated with the T-M transformation cause microcracking in the PSZ ceramic coating during cyclic oxidation[9-11]. The repeated thermal cycling of PSZ ceramic coating through the transformation temperature will cause extensive microcracking and results in the degradation of the PSZ ceramic coating.

Previous studies showed that a large quantity of microcracks formed by the T-M transformation caused the strength and toughness to decrease for the zirconia ceramic materials[12]. In addition, the networks of interconnected cracks formed by the T-M transformation provide path for oxygen transport, resulting in the oxidation of bond coat. The extent of degradation due to the T-M transformation would depend on the amount of transformable T phase(i.e. amount of transformed M phase at room temperature) present in the PSZ ceramic coating. Thus the phase distribution in a PSZ ceramic coating would be a critical design parameter. A tolerable amount of the transformable T phase for the superior durability of PSZ coatings has not yet been established. But an optimum amount of yttria in zirconia at which the longest life was obtained has been reported to be 6 to 8 wt.%[1-4].

Although ZrO_2-Y_2O_3 coatings currently provide adequate service life when exposed to clean fuel flames, these coatings are destabilized in vanadium and SO_2 containing environments due to the formation of a vanadium-yttrium compound and leaching of yttria from PSZ[13, 14]. It is known that ZrO_2-CeO_2 coatings are more resistant to hot corrosion than ZrO_2-Y_2O_3[15]. Thus in this study, phase stability was characterized on the plasma sprayed zirconia coatings stabilized with CeO_2 ranging from 16 to 26 wt. % to determine the effect of phase transformations on the durability of the coatings. The selection of these compositions was based on the phase diagram for the ZrO_2-CeO_2[16]. The phase analysis was performed in the as-deposited state and after thermal cyclic oxidation using X-ray diffraction.

2. Experimental Procedure

Disk-shaped(25㎜ diameter by 3㎜ thick) nickel base superalloy(Rene'N4) specimens were prepared for two layer thermal barrier coatings. 125㎛ thick NiCoCrAlY bond coats and 330㎛ thick PSZ ceramic coatings were deposited by vacuum plasma spraying and air-plasma spraying, respectively. The spray parameters used for TBC deposition are seen in Table 1. The composition of the bond coat is Ni-4Co-9Cr-6Al-0.3Y(in wt.%). The PSZ ceramics with compositions of ZrO_2 with 16, 18, 20, 22, 24 and 26 wt. % CeO_2 were used for the ceramic coating. Chemical Analysis for the ZrO_2-CeO_2 are given in Table 2. Particle size distributions for the NiCoCrAlY bond coats and the ZrO_2-CeO_2 powders are -230 to +400 mesh and -200 to +325 mesh, respectively. Prior to the PSZ ceramic coating application, the bond

Table 1. Plasma Spray Deposition Parameters for ZrO_2-CeO_2 Coating

Parmeters	Conditions
Current(A)	500
Voltage(V)	75
Plasma Gas	Primary - N_2
	Secondary - H_2
Gas Pressure(KPa)	Primary - 345
	Secondary -345
Spray Distance(cm)	12.7
Spray Rate(Kg/hr)	3.6

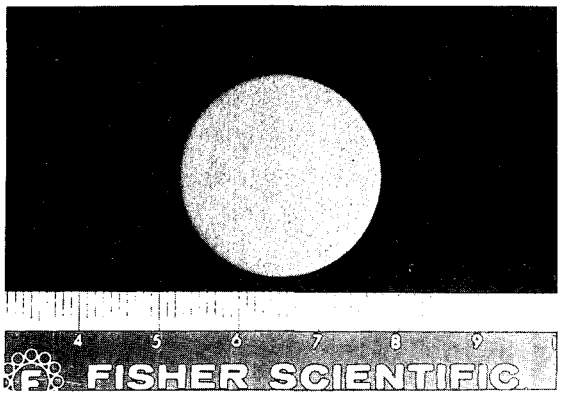

Fig. 1a-As-deposited Specimen

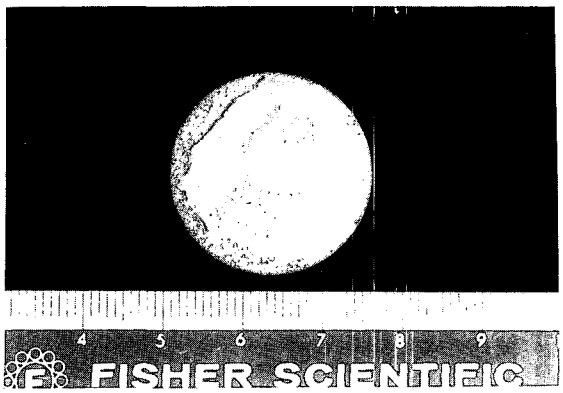

Fig. 1b-Themally Cycled Specimen

Table 2. Chemical Analysis of ZrO_2-CeO_2 Powders Used for This Study

Ceramic Oxide	Composition(wt. %)							
	CeO_2	CaO	MgO	SiO_2	Fe_2O_3	Al_2O_3	TiO_2	ZrO_2
ZrO_2 - 16 CeO_2	16.35	0.27	0.08	0.73	0.29	0.06	0.04	Bal
ZrO_2 - 18 CeO_2	18.23	0.26	0.07	0.74	0.12	0.06	0.04	Bal
ZrO_2 - 20 CeO_2	20.01	0.25	0.10	0.77	0.02	0.05	0.04	Bal
ZrO_2 - 22 CeO_2	21.86	0.24	0.07	0.69	0.10	0.06	0.04	Bal
ZrO_2 - 24 CeO_2	23.88	0.23	0.06	0.70	0.03	0.05	0.04	Bal
ZrO_2 - 26 CeO_2	25.98	0.22	0.06	0.68	0.03	0.04	0.03	Bal

coats were pack aluminized (Codep B-1 Process) to improve oxidation resistance[17].

To investigate phase stability of the PSZ ceramic coating during their lifetimes, the as-deposited specimens were exposed to the cyclic oxidation conditions. The cyclic oxidation tests were carried out every 65 minutes from 200℃ to 1135℃ at atmospheric pressure in a furnace. The 65 minute thermal cyclic oxidation test consisted of a 10 minutes heat-up from 200℃ to 1135℃, a 45minute hold at 1135℃, followed by cooling to 200℃ in 10 minutes. This procedure was repeated from 230 to 340 cycles, until the specimens showed at least 10% coating spallation. Coatings were considered failed when they showed 10% ceramic coating spallation The as-deposited and the thermally cycled specimens are seen in Figures 1a and 1b, respectively.

The quantitative phase analysis for the as-deposited and heat treated PSZ coatings were carried out by X-ray diffration with monochromated CuKα radiation. The step scan technique was used at 0.05° interval in 2θ and with a fixed counting time of 10 seconds. Two regions of X-ray diffraction were analyzed to estimate the propotions of the cubic, tetragonal and monoclinic phase. In the first region(26° to 34° in 2θ), the ratio of the intergrated intensi

ties of the $(11\bar{1})$ and (111) monoclinic peaks to those of the (111) cubic and nearly coincident (111) tetragonal peaks was determined. In the other region(70° to 77° in 2θ), the ratio of the integrated intensity of the (400) cubic peak to the integrated intensities of the (400) plus (004) tetragonal peaks was also determined. The fraction of each phase was calculated from the equation below[18, 19].

$$\frac{M_m}{M_{t+f}} = 1.39\,\frac{I_m(11\bar{1}) + 1_m(111)}{(I_{t+f})}$$

$$\frac{M_f}{M_t} = \frac{I_f(400)}{I_t(400) + I_t(004)}$$

$$M_t + M_f + M_m = 1$$

where M_t, M_f and M_m are the mole fraction of the tetragonal, cubic and monoclinic phases, respectively. I_t, I_f and I_m are the integrated X-ray intensities of the tetragonal, cubic and monoclinic peaks, respectively. Since the (400) cubic peak is centered between the two tetragonal peaks in the (400) region, deconvolution of the (400) peaks was performed using a computer model develoed by Douglas[18]. The integrated intensity of each peak, which is the area under the peak, was also caculated using the computer model[18].

3. Results and Discussion

3. 1 As-deposited ZrO_2-CeO_2 Coatings

Figures 2a and 2b present the SEM photomicrograph for the top surface of the as-deposited and the thermally cycled ceramic coatings, respectively. As seen in Figure 2a, the as-deposited PSZ ceramic coating is observed to consist of layed structure with cracks on the top surface. It is found that no monoclinic phase exists in the as-deposited PSZ coating with 16 to 26 wt. % CeO_2. In the X-ray diffraction patterns in the (111) region, no differences were found among the PSZ ceramic coatings with different composition. Thus the results of the X-ray diffraction patterns in the (111) region are presented for two samples(ZrO_2 with 16 and 26 wt. % CeO_2) in Figure 3. The X-ray diffratction patterns in the (400) region for the as-de

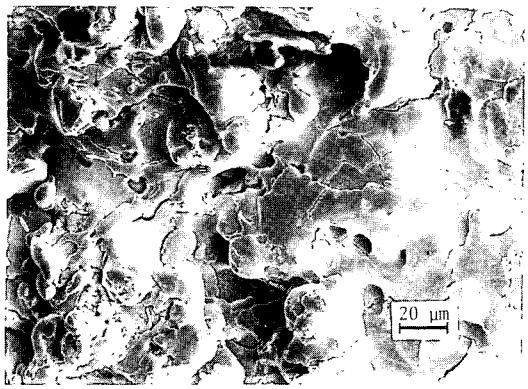

Fig. 2a-SEM Photomicrograph for the Top Surface of the As-deposited Caramic Coating

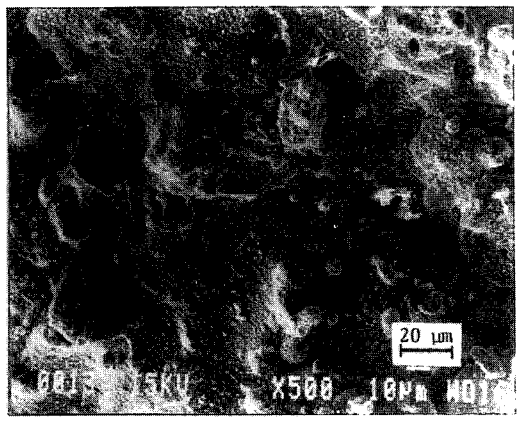

Fig. 2b-SEM Photomicrograph for the Top Surface of the Themally Cycled Ceramic coating

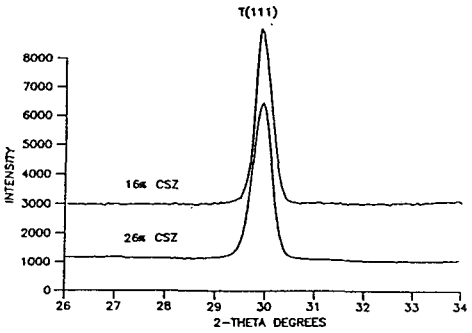

Fig. 3-X-ray Diffraction Patterns in the (111) Region for the As-deposited PSZ Coatings with 16 and 26 wt. % Ceo_2

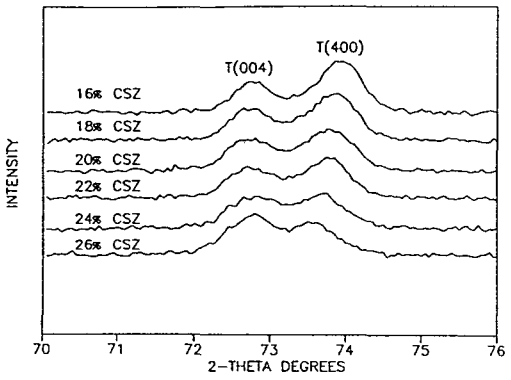

Fig. 4-X-ray Diffraction Patterns in the (400) Region for the As-deposited PSZ Coatings with 16 and 26 wt.% CeO_2

posited PSZ coating are presented in Figure 4. It is observed that the angular seperation between (004) and (400) peaks decreases with increasing CeO_2 content as seen in Figure 4. In addtion, the relative intensity of (004) peak increases with increasing CeO_2 content, indicating that the intensity of the (400) cubic peak between (004) and (400) tetragonal peaks increases with increasing CeO_2 content. Deconvolution of each X-ray diffraction pattern on Figure 4 was carried out using the computer model called DECON[18]. One of the deconvolution products of DECON is seen in Figure 5. Based on the deconvolution of peaks in the (400) region, the as-deposited PSZ coatings with 16 and 18 wt. % CeO_2 are determined to consist of only tetragonal phase while the PSZ coating with 20 to 26 wt. % CeO_2 consist of a mixture of the cubic phase and the tetragonal phase as seen in Figure 4.

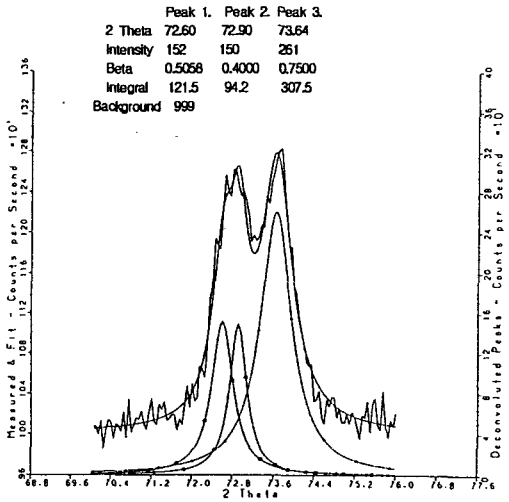

Fig. 5-Deconvoluted X-ray Diffraction peaks in the (400) Region for the As-deposited PSZ Coatings with 24 wt.% CeO_2

The lattice parameters(a or/and c) for the tetragonal phases as well as the cubic phases developed in the as-deposited PSZ coatings were calculated from the X-ray diffraction peak positions. The calculated lattice parameters for the tetragonal and the cubic phases are prtesented in Table 3. In Table 3, the lattice parameters (a and c) for the tetragonal phases are seen to increase with increasing CeO_2 content in the PSZ coatings. The ratios of c/a for the tetragonal phases are seen to vary between 1.0115 and 1.0137. These values are much less

than the c/a value for the equilibrium tetragonal phase(1.0190) at 1150 ℃[16]. This result indicates that the tetragonal phases developed in the as-deposited PSZ coatings are non-equilibrum, high-ceria tetragonal phases(T′). As seen in Table 3, the lattice parameter(a) for the cubic phase increases with increasing CeO_2 content, since the ionic radius of Ce^{+4}(0.94Å) is larger than that of Zr^{+4}(0.79Å). This result suggests that the cubic phases(F′) observed in the as-deposited PSZ coating are non-equilibrium, low ceria phases(i.e. a retained cubic phase). Thus it can be said that for the as-deposited PSZ coatings with 16 and 18 wt.% CeO_2 the high temperature cubic phase transformed totally to the non-equilibrium tetragonal phase (T′) by a diffussionless phase transformation while for the as-deposited PSZ coating with 20 to 26 wt. % CeO_2 the high temerature cubic phase transformed to the mixture of the T′ phase and the F′ phase during the plasma spraying. This result indicates that the maximum concentration of CeO_2 in the high temperature cubic phase requried for the complete transformation from the cubic to the non-equilibrium tetragnal(T′) phase is between 18 to 20 wt. % CeO_2.

The mole fraction of each phase developed in the as-deposited PSZ coatings with various amount of CeO_2 was calculated using the equations described in the previous section. The calculated mole fraction of each phase is presented in Table 4.

3. 2. Thermally Cycled ZrO_2-CeO_2 Coatings

The X-ray diffraction patterns in the (111) region for the top surfaces of the thermally cycled PSZ coatings with 16 to 26 wt. % CeO_2 are similarly shaped but differ only in the relative intensity of each peak. The typical examples of the X-ray diffraction patterns for the thermally cycled PSZ coatings(ZrO_2 with 16 and 26 wt. % CeO_2) are seen in Figure 6. As seen in this figure, monoclinic phase developed after cyclic oxidation. It is observed that a large quantity of monoclinic phase developed in the PSZ coating with 16 wt. % CeO_2 (17 mole%)

Table 3. Lattice Parameters for the Tetragonal and the Cubic Phases Developed in the As-deposited and the Thermally Cycled PSZ Coatings

CeO_2	AS-DEPOSTED				THERMALLY CYCLED			
	TETRAGONAL			CUBIC	TETRAGONAL			CUBIC
(wt.%)	a	c	c/a	a	a	c	c/a	a
16	5.1293	5.1995	1.0137	*	5.1192	5.2149	1.0187	5.3772
18	5.1364	5.2019	1.0128	*	5.1209	5.2180	1.0190	5.3697
20	5.1382	5.2063	1.0133	5.1866	5.1233	5.2218	1.0192	5.3788
22	5.1394	5.2050	1.0128	5.1909	5.1209	5.2199	1.0193	5.3788
24	5.1460	5.2093	1.0123	5.1909	5.1202	5.2173	1.0191	5.3607
26	5.1514	5.2106	1.0115	5.1970	5.1203	5.2211	1.0197	5.3697

* : Cubic phase was not observed in the as-deposited ZrO_2-16 wt%CeO_2 and ZrO_2-18 wt%CeO_2

Table 4 Measured Mole Fraction of Each Phase Developed in the As-deposited and the Thermally Cycled PSZ Coatings

CeO_2	AS-DEPOSTED				THERMALLY CYCLED			
(wt.%)	T′	F′	F	M	T	F′	F	M
16	1.0	0	0	0	0.82	0	0.01	0.17
18	0.98	0	0	0	0.94	0	0.03	0.03
20	0.94	0.06	0	0	0.89	0	0.05	0.06
22	0.93	0.07	0	0	0.85	0	0.06	0.09
24	0.84	0.16	0	0	0.88	0	0.10	0.02
26	0.74	0.26	0	0	0.86	0	0.12	0.02

T : Equilibrium Tetragonal Phase with Low CeO_2 Content
T′ : Non-Equilibrium Tetragonal Phase with High CeO_2 Content
F′ : Non-Equilibrium Cubic Phase with Low CeO_2 Content
F : Equilibrium Cubic Phase with High CeO_2 Content
M : Monoclinic Phase

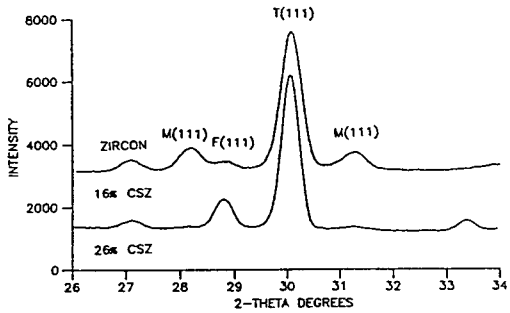

Fig. 6-X-ray Diffraction Pattems in the (111) Region for the Thermally Cycled PSZ Coatings with 16 and 26 wt.% CeO_2

while less monoclinic phase developed in the PSZ coatings with 18 to 26 wt. % CeO_2 (2 to 9 mole.%). This effect could be a result of larger grain size at the lower concentration of CeO_2 in ZrO_2. For the ZrO_2-16 wt. % CeO_2 coating, 10 % ceramic coating spallation occured after 230 thermal cycles while for the PSZ coatings with 18 to 26 wt. % CeO_2, 10% spallation occured in 320 to 340 thermal cycles. Thus it is considered that the tolerable amount of CeO_2 in PSZ coating for TBC is above 16 wt. %. In addition, (111) cubic peaks are observed in the (111) region of the X-ray diffraction as seen in Fingure 6.

A predicted plot of CeO_2 concentration in ZrO_2-CeO_2 alloys vs lattice parameter of cubic phase based on Vegard's Law is presented in Figure 7. In this plot, the lattice parameter, a for cubic ZrO_2 alloy was assumed to increase linearly with increasing CeO_2 content in ZrO_2 alloy. Thus the values of the lattice parameters, a for the cubic ZrO_2 and the cubic CeO_2 were linearly connected as seen in Figure 7. The predicted plot is in good agreement with the experimental data measured by Tani, et al[16]. Based on the predicted plot as seen in Figure 7, the concentration of CeO_2 in the cubic phases developed after cyclic oxidation is estimated to be approximately 85 wt.%. This valuecorres-ponds closely to the equilibrium cocentration on the

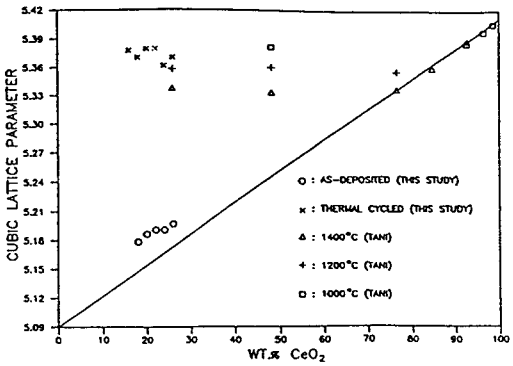

Fig. 7-Comparison of the Predicted and the Experimerimental Cubic Lattice parame. tera of ZrO_2-CeO_2 Alloys

the solvus line(T+F/F) at 1150℃ in the equilibrium binary ZrO_2-CeO_2 phase diagram[16]. Thus the cubic phase develpoed in the thermally cycled PSZ coatings is the equilibrium cubic phase. As seen in Figure 6, some zircon($ZrSiO_4$) has developed in the thermally cycled PSZ coating. The Si was supplied from the molybdenum disilicide heating elements of the furnace.

The X-ray diffraction patterns in the (400) region for the thermally cycled PSZ coating with 16 to 26 wt. % CeO_2 are observed to be same. The X-ray patterns for the PSZ coatings with 16 and 26 wt. % CeO_2 are presented in Figure 8. As seen in this figure, only (004) and (400) tetragonal peaks are seen for the thermally cycled PSZ coatings. The lattice parameters(a and c) for the tetragonal(T) phases in the thermally cycled PSZ coatings are contant with increasing content of CeO_2 as seen in Figure 9. This result indicates that the tetragonal phases developed after cyclic oxidation(230 to 340 cycles) are the equilibrium tetragonal phases with low CeO_2 content. The lattice parameters of these tetragonal phases are in good agreement with the equilibrium values given by Tami, et al[16] for the slightly higher temperature of 1200℃.

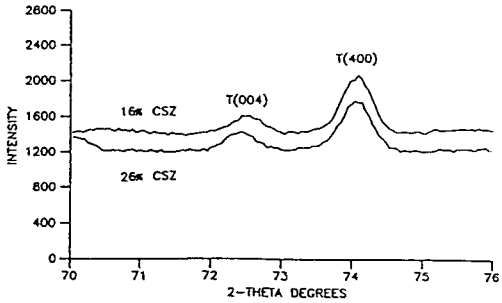

Fig. 8-X-ray Diffraction patters in the (400) region for Thermally Cycled PSZ Coatings with 16 and 26 wt.% CeO_2

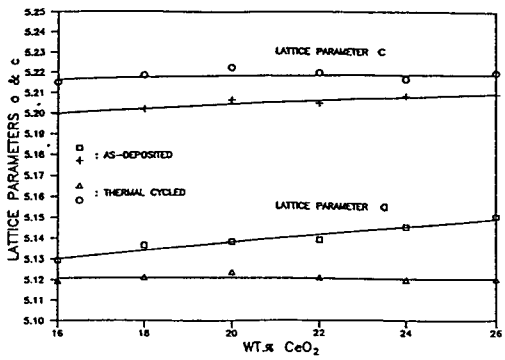

Fig. 9-Plot of the Lattice Parameters for the Tetragonal Phase against CeO_2 Content in the As-deposited and the Thermally Cycled PSZ Coatings

Based on the X-ray diffraction patterns in the two regions, the thermally cycled PSZ coatings are determined to consist of equilibrium tetragonal(T)(with low CeO_2 content), equilibrium cubic(with high CeO_2 content) and monoclinic phases. Thus it can be said that the non-equilibrium tetragonal(T′) phases(or the mixture of T′ and the non-equilibrium cubic phase) present in the as-deposited PSZ coating decom-posed to the equilibrium tetragonal(T) phase and the equilibrium cubic(F) phase dur

ing cyclic oxidation. Some of the tetragonal(T) phase transformed to the monoclinic phase upon cooling. The measured mole fraction of each phase developed in the thermally cycled PSZ coatings is presented in Table 4.

It was observed that little monoclinic phase has developed on the bottom surfaces(i.e. surfaces attached to the metal) of the PSZ ceramic coating while a significant quantity of monoclinic phase has developed on the top surfaces. One of the X-ray diffraction patterns in the (111) and (400) regions compared between the top and bottom surfaces of the PSZ coatings with 22 wt.% CeO_2 is presented in Figures 10 and 11. This diffrence may be due to the different average grain size or stress state on both surfaces.

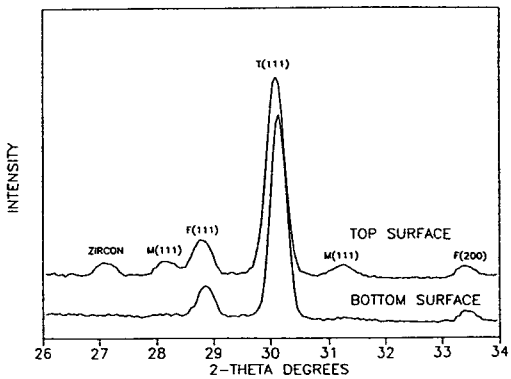

Fig. 10-Comparison of the X-ray Diffraction Pattems in the (111) Region for the Top and the Bottom Surfaces of the Spalled ZrO_2-22 wt.% CeO_2 Coating

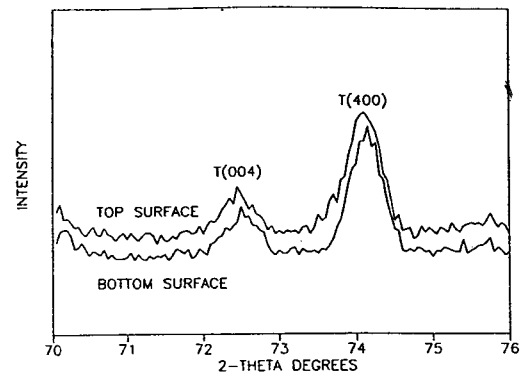

Fig. 11-Comparison of the X-ray Diffraction Pattems in the (111) Region for the Top and the Bottom Surfaces of the Spalled ZrO_2-22 wt.% CeO_2 Coating

4. Conclusions

1) The results of the phase analysis showed that the as-sprayed PSZ coatings with 16 and 18 wt. % CeO_2 consist of only non-equilibrium tetragonal(T′) phase (with high CeO_2 content) while the PSZ coatings with 20 to 26 wt. % CeO_2 consist of a mixture of T′ and some amount of non-equilibrium cubic(F′) phase (with low CeO_2 content). Thus the maximum concentration of CeO_2 in the high temperature cubic phase reguired for the complete transformation from the cubic to the T′ phase would be between 18 and 20 wt. %.

2) During cyclic oxidation(230 to 340 cycles), the T′ phase as well as the mixture of T′ and F′ decomposed to equilibrium cubic(F) phase(with high CeO_2 content) and equilibrium tetargonal(T) phase(with low CeO_2 content). Some of the T phase transformed to the monoclinic phase upon cooling. More monoclinic phase developed on the top surface than the bottom surface of the PSZ ceramic coating during cyclic oxidation. Less monoclinic phase developed in the PSZ coatings with 18 to 26 wt. % CeO_2 (less than 10 vol.%) than the PSZ coating with 16 wt. % CeO_2(17 vol.%)

3) For the PSZ coating with 16 wt. % CeO_2, 10% ceramic coating spallation occurred after

230 cycles while the PSZ coatings with 18 to 26 wt. % CeO_2 occurred in 320 to 340 cycles. The difference in the lifetimes of the PSZ coatings would be resulted from the different amount of tranformable T phase(which is observed as monoclinic phase at room temperature). Thus the tolerable amount of CeO_2 in ZrO_2 alloy required for TBCs would be more than 16 wt. %.

Acknowledgement

This research has beem supported by Non Directed Research Fund, Korea Research Foundation in 1994. The author is also thankful to Prof. J. W. Holmes in Dep't of Materials Science and Engineering, University of Michigan for providing the samples.

References

1. R.A.Bratton and C.E.Lowell : Science and Technology, 3(1981) 226
2. R.A.Miller and C.E.Lowell : Thin Solid Films, 95(1982) 265
3. J.A.Colwell : Report by Metals and Ceramic Information Center, MCIC-86-C2(1986)
4. D.J.Wortman, B.A.Nagaraj and E.C.Duderstadt : Materials Science and Engineering, A121(1989) 437
5. R.A.Miller : Surface and Coatings Technology, 30(1987) 1
6. C.E.Youngblood : Journal of American Ceramic Society, 71(1988) 225
7. J.R.Brandon and R.Tayler : Surface and Coatings Technology, 39(1989) 143
8. C.C.Berndt : Thin Solid Films, 108(1983) 1
9. A.H.Heuer : Journal of the American Ceramic Society, 70(1987) 689
10. F.F.Lange : Journal of Materials Science, 17(1982) 240
11. F.F.Lange, G.L.Dunlop and B.I.Davis : Journal of the American Ceramic Society, 69(1986) 237
12. R.L.K.Matsumoto : Journal of the American Ceramic Society, 71(1988) 128
13. S.Stecura : Thin Solid Films, 150(1987) 15
14. R.L.Jones, C.E.Williams and S.R.Jones : Journal of Electrochemical Society, 133 (1986) 227
15. D.W.Mckee and P.A.Siemers : U.S. Patent 4328285(May 1982)
16. E.Tani, M.Yoshimura and S.Somia : Journal of the American Ceramic Society, 66(1983) 506
17. J.W. Holmes, F.A.McClintock, K.S. O'Hara and and M. Conners : Low Cycle Fatigue Testing of Coated Monocrystalline Superalloys, (1988) 672
18. C.Douglas : MS Thesis, Worcester Polytechnisc Institute(1987) 35
19. R.A.Miller : Science and Technology of Zirconia, 3(1981) 241